851. Entropy-based fault detection approach for motor vibration signals under accelerated aging process

D. Sonmez[1], S. Seker[2], M. Gokasan[3]
Faculty of Electrical and Electronic Engineering, Istanbul Technical University
34469, Maslak, Istanbul-Turkey
Email: [1]*duhansonmez@itu.edu.tr*, [2]*sekers@itu.edu.tr*, [3]*gokasan@itu.edu.tr*

Abstract. The purpose of this study is to analyze motor vibration signals due to the bearing fault, which is artificially generated by aging process. Vibration signal data recorded by the experimental setup has been conditioned by a high-pass filter (Butterworth type) to reach the regarding frequency components of the bearing failure. Spectral analysis has been applied to realize the degradation on the bearing and the power spectral density figures revealed that the magnitudes of frequency components between 1.5-4 kHz bandwidth increased after every aging cycle. Vibration signals were investigated statistically by examining four main statistical parameters: mean value, standard deviation, skewness and kurtosis. Evaluation of these parameters indicated that significant variance occurred on standard deviation. At this point Shannon entropy became an approach to analyze the variance on the standard deviation. The probability of the aging cycles has been defined as a function of standard deviation values for each aging cycle. Entropy definition, which is a function of probability, determines the uncertainty level on the data and it has been examined to identify the effect of the aging progress on the bearing by examining the transferred entropy amount between aging cycles.

Keywords: motor vibration signal, bearing fault, spectral analysis, statistical analysis, aging process, Shannon entropy.

1. Introduction

The usage of induction motors in recent decades increased evidently in various industries. The main reasons depend on the facts of easy structure and running facilities, low cost and maintenance efforts and high reliability. On the other hand, the performance goals in every industry started to force the enterprises to increase the productivity efficiency by minimum failure at these production lines, which means that every motor has to run without fault continuously. Therefore, this approach increased the importance of fault diagnosis tools and applications for induction motors significantly. According to the studies on this subject in [1-5], it is observed that the most significant motor faults are because of the mechanical effects. In particular, bearing faults take an important part (more than 40 % of all induction motor faults). Also many researchers concentrated on the development of fault diagnosis and condition monitoring techniques to detect incipient motor faults signals and overcome the unscheduled machine down-times because of motor faults.

There are many different approaches and techniques developed in recent decades, which are mainly based on three groups as "Signal-based", "Model-based" and "Data-based" condition monitoring and fault diagnosis techniques. Signal-based fault signature analysis is one of the most preferred techniques for condition monitoring and diagnosis and also to investigate the incipient fault signature of the motor. There are different types of signals that can be measured and analyzed from the actual motor which has been subjected in [1-5]. Mainly these are electrical measurements (current, power, flux), mechanical measurements (vibration, noise), temperature measurement, chemical measurements (gas analysis) and partial discharge detection.

Bearing faults generally causes static and dynamic eccentricities on the rolling elements, which lead to many negative effects on the performance of the motor. Primarily, mechanical vibration on the system occurs due to bearing faults and the level of the signal increases during

1263

the fault progress as mentioned in [6-8]. Therefore, this study concentrates on vibration signal analysis for an AC motor. A proper aging process is applied at seven sequential steps for this motor, to bring out the bearing fault and its effects at the end of this period. Measured actual motor vibration signals will be investigated for each aging cycle by spectrum analysis and statistical parameters, which will be helpful to diagnose the status of the motor bearing and follow up the aging process in terms of bearing degradation trend.

Shannon Entropy definition, which explains the amount of uncertainty on a random signal, will be implemented in this study to get the data flowing through the aging process, from healthy case to the bearing fault case as mentioned in [9]. This approach will be helpful to understand the level of fault in the aging process. The amount of entropy variation between each aging cycle, which is called as entropy transfer rate in this study, will be evaluated to be able to determine the degree of degradation in the motor bearing.

2. Aging Process by Stochastic Entropy

The cascade steps in an aging system accelerate the physical system collapse. This mechanism can be illustrated by Fig. 1 in terms of linear system approach.
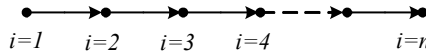

Fig. 1. Aging in a linear structured system

Each node of the cascaded aging process defines the probability values of the aging steps. Hence while the physical system becomes old, the probability value of functioning p_i slopes down [10]. This trend describes the entropy in this system as:

$$H_i = H(p_i) \tag{1}$$

Therefore stochastic entropy shows that the failure risk of the system increases during the aging process. From that point of view, entropy differences between two sequential points can be defined by following expression:

$$\Delta H_i = H_i - H_{i-1} \tag{2}$$

where i is the node number as in Fig. 1. Thus, the change of the entropy difference according to the change of probability value defines the slope of the trend in the system as given below:

$$\frac{\Delta H_i}{\Delta p_i} \cong \tan \alpha \tag{3}$$

This trend is in the direction of decreasing, while probability value difference varies with the time as $\Delta p_i \propto t$. Therefore the entropy difference can be given as:

$$\Delta H_i = -\lambda_i \cdot t \tag{4}$$

This is the entropy of the generic component i, in the aging step of A_i, for $\lambda_i > 0$. As a result, the stochastic entropy $H(A_i)$ is a function of the probability p_i of the state A_i:

$$H(A_i) = H(p_i) = \log_e(p_i) \tag{5}$$

3. Motor Bearing Faults and Experimental Setup for Accelerated Aging Process

3.1 EDM Effect on Motor Bearing

There are many reasons that cause bearing faults which are mainly based on electrical and mechanical effects. One of the most important reasons for degradation of bearings is electrical

discharge mode current, which is flowing from motor shaft to the ground throughout bearing elements. The effect of this faulty current is known as Electrical Discharge Machining (EDM).

The reasons of the discharge mode current depend on the bearing voltage which is generally increased by electrostatic loads and non-symmetrical magnetic circuitry of the motor, also high frequency switching (PWM) inverters, which are very common in industrial applications, cause the same bearing voltage and discharge mode current [11, 12].

A motor bearing has a structure covering the elements of outer race, inner race, rolling elements (ball, cylinder, etc.) and a raceway. The grease, being used inside the cage of bearing, is normally between the rolling elements and the races, and it is not conductive. During the motor operation at high speeds, the grease forms a uniform distributed layer between bearing rolling elements and races, thus the rotor voltage increases up to a level with respect to ground. When the voltage reaches critical level, an intermittent discharge current with arching will flow from the body to the ground, over the bearing rolling elements. If the rolling speed of the motor is slow, then the grease thickness will be minimum, which will cause a direct conduction between rolling elements and races. The rotor voltage will not increase because of the current continuously flowing over bearing to the ground. Therefore there appear two different types of bearing current; as conductive mode current (continuous) and discharge mode current (arching). Discharge mode current causes negative effects on the bearing elements as surface degradation. Commonly known defects are "pitting" and "fluting", which start with primitive damage and continues with growing level of noise and vibration, finally leading to bearing fault.

3.2 Experimental Setup for Aging Process

An experimental setup was designed to simulate the aging process for a 5HP AC motor, which is under electrical and mechanical stresses, also thermal and corrosive effects are added to this artificial aging process. This experimental setup is designed regarding IEEE Standard Test Procedure for AC Electrical Machinery and Standard for Systems of Insulation Materials [13, 14].

Electrical and thermal aging processes are applied sequentially to the test motor as an aging cycle and this cycle is repeated seven times totally as described in [15, 16].

Each aging cycle starts with Electrical Discharge Machining (EDM) process in order to simulate electrical discharge current from motor shaft to the bearing. The designed test set for this facility is shown in Fig. 2. At each EDM aging cycle the motor was run for 30 minutes with no load condition and during the period, an externally supplied shaft current (27 A at 30 VAC) is applied to the motor shaft.
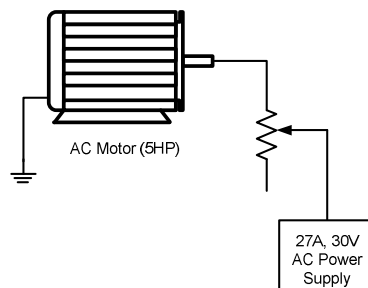

Fig. 2. EDM setup for the AC motor

After each EDM aging cycle, a thermal aging process was carried out, which was applied to accelerate the aging process. Basically in a thermal aging process, the motor is heated up in a laboratory oven that gives a constant temperature of 140°C, and after the heating process, it is immersed in the water. The cycle is repeated again after waiting in water to expose the corrosion effect on the motor components.

Each aging period was followed by a performance test process on an experimental setup, where high frequency data was collected with respect to motor currents, voltages, rotor speed, and six vibration measurements at a sampling frequency of 12 kHz. Eventually eight set of measurements are performed as one healthy and seven aged cases.

The experimental setup, shown in Fig. 3, covers electrical and mechanical vibration measurement instruments, signal conditioner and the host personal computer. There are two accelerometers in this setup for independent vibration measurements and the locations of the two accelerometers, S1 and S2, are in plane 'A-B' of the motor at process end, on clock position by 2 and 10 respectively. After getting the vibration signal from accelerometers, signal conditioners with anti-aliasing filter are used before data process in a host PC. The anti-aliasing filter has been set to 4 kHz cut-off frequency.
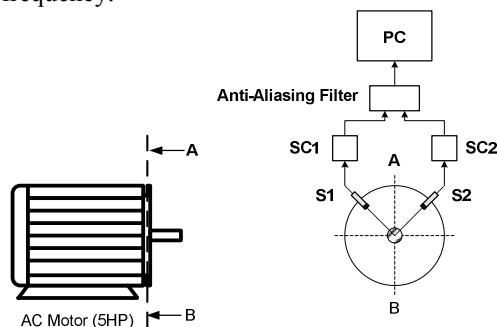

Fig. 3. Data collection set: accelerometers S1 and S2 in motor plane A-B for vibration measurement

4. Data Analysis for Vibration Signals

The mathematical fundamentals regarding the vibration signal analysis by spectral analysis and statistical analysis can be found in the Appendix A.

In this study, eight sets of vibration signal data has been recorded with a sampling rate of 12 kHz for ten seconds by S2 accelerometer, at 100 % load condition of the test motor. The first set is for initial (healthy) motor condition and the other seven sets belong to the aging cycles respectively.

The test motor is a 5HP, three-phase, four-pole induction motor. There is an anti-aliasing filter which is set at 4 kHz cut-off frequency.

4.1 Spectral Analysis

The first inspection due to each aging cycle data has been in time domain and it was observed that vibration signal magnitude increases during the degradation period in the aging process, which is shown in Fig. 4. This increase gives an idea about degradation of bearing but it does not give some characteristic details about aging process and the bearing fault.

Therefore when the vibration signal has been examined by spectral analysis, Power Spectral Density (PSD) plot, given in Fig. 5 indicates that there are additional frequency components after 1.5 kHz, which points out a bearing fault trend during the aging process.

It is also possible to realize the deviation on vibration signal data, by looking at PSD plot in logarithmic scale as shown in Fig. 6. It is obvious that the subjected deviation arises after frequency level of 1.5 kHz.

Because of the additional frequency components in the range of 1.5-4 kHz on the spectrum, it was decided to investigate only this frequency range, just to ignore the effect of low frequency components during spectrum analysis. Therefore a Butterworth type of high-pass filter has been

applied to the signal. This high-pass filter is a 5th order filter, which is set to 1.5 kHz cut-off frequency.
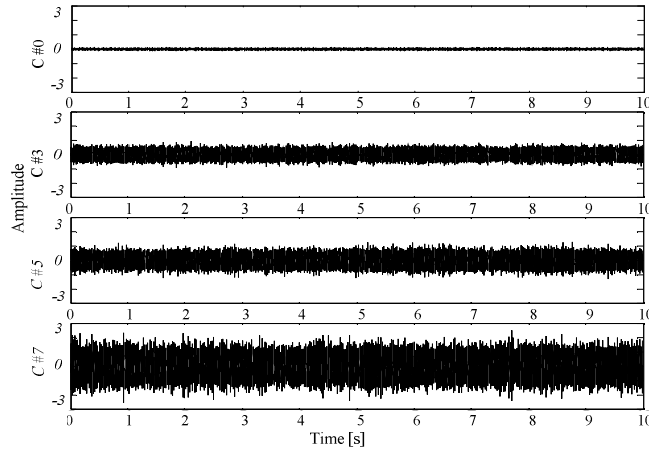

Fig. 4. Time domain amplitude plots of vibration signal for aging cycle No #0, 3, 5 and 7
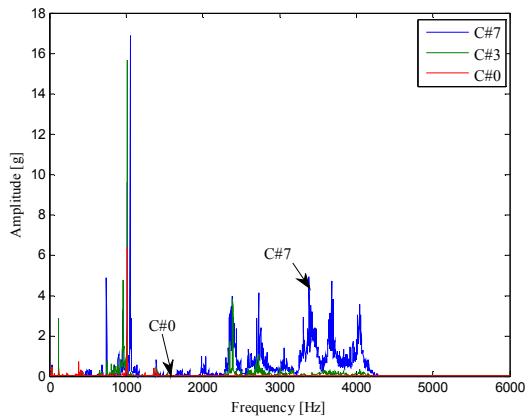

Fig. 5. PSD comparison of aging cycles in the frequency domain (unfiltered data)
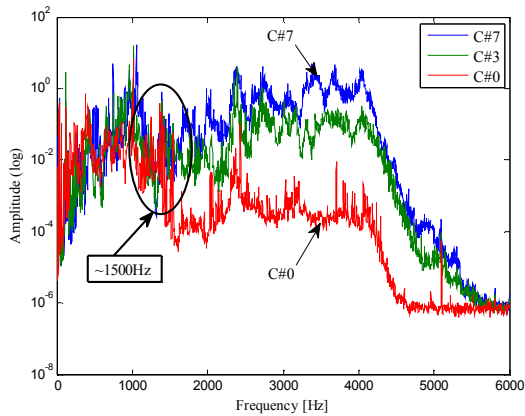(Case #0 - Healthy motor, Case #3 and Case #7 - Bearing fault)

Fig. 6. PSD comparison in logarithmic scale (unfiltered data)
(Case #0-Healthy motor, Case #3 and Case #7-Bearing fault)

1267

After filtering out lower frequency components by Butterworth type high-pass filter, the frequency spectrum of the vibration signal has been plotted (Fig. 7) for initial healthy case and other three aging cycles. The figure reveals the increasing frequency components by each aging cycle.
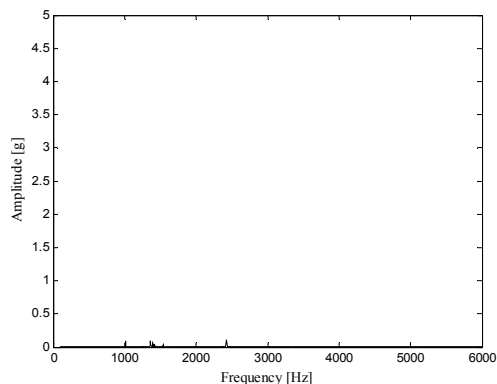
Fig. 7(a). PSD comparison of aging cycles in frequency domain (high-pass-filtered data)
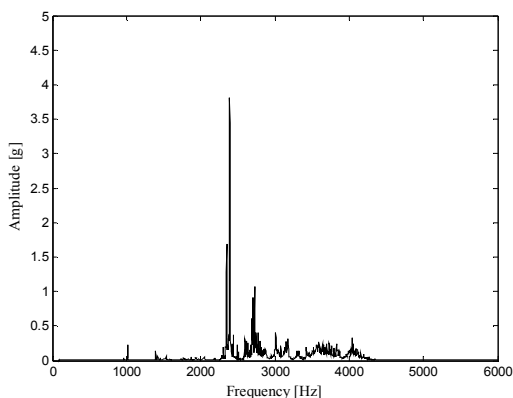(Case #0 - Healthy motor, Case #3 and Case #7 - Bearing fault)

Fig. 7(b). PSD comparison of aging cycles in frequency domain (high-pass-filtered data)
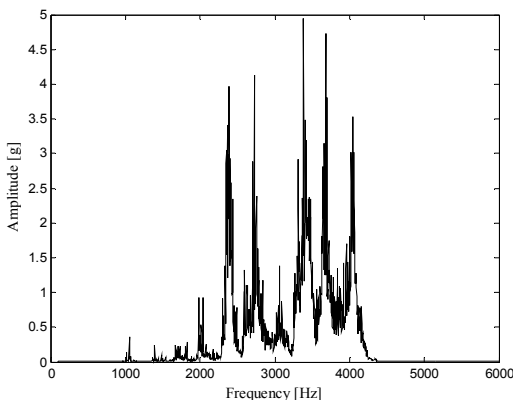(Case #3 - Aging Cycle #3)

Fig. 7(c). PSD comparison of aging cycles in frequency domain (high-pass-filtered data)
(Case #7 - Bearing fault)

It was revealed that high frequency components above 1.5 kHz are increased after each aging cycle therefore this indicates the degradation of the bearing.

When the PSD plots are compared in logarithmic scale (Fig. 8), the increase of the magnitude of high frequency signal components by each aging cycle clearly points out the degradation of the bearing.
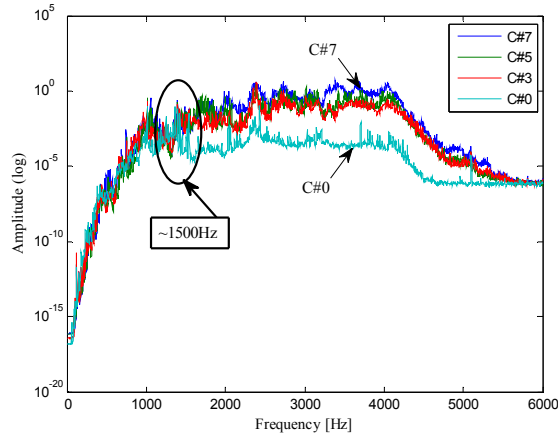

Fig. 8. PSD comparison in logarithmic scale (high-pass-filtered data)
(Case #0 - Healthy motor, Case #3 and Case #7 - Bearing fault)

4.2 Statistical Analysis

Statistical parameters, which are defined in Appendix B, are mean value (μ), standard deviation (σ), skewness (α) and kurtosis (β). They have been calculated for each aging cycle to analyze the vibration signal data. Table 1 lists the values of these parameters.

Table 1. Values of statistical parameters for each aging cycle

Aging Cycle	Mean Value (μ)	Standard Deviation (σ)	Skewness (α)	Kurtosis (β)
C#0	$-2,68.10^{-7}$	0,0267	$-8,18.10^{-2}$	3,2874
C#1	$-9,83.10^{-7}$	0,0642	$1,53.10^{-5}$	3,2741
C#2	$3,65.10^{-7}$	0,1355	$-3,85.10^{-4}$	3,1475
C#3	$-8,74.10^{-7}$	0,2127	$1,70.10^{-7}$	3,0662
C#4	$3,70.10^{-7}$	0,2980	$-3,46.10^{-4}$	3,0398
C#5	$-5,40.10^{-7}$	0,2953	$-8,35.10^{-4}$	3,0303
C#6	$-3,56.10^{-6}$	0,3576	$-1,60.10^{-3}$	3,0207
C#7	$4,96.10^{-6}$	0,5578	$-9,33.10^{-4}$	3,0366

For the healthy motor, the vibration signal data draws a standard normal (Gaussian) distribution in terms of probability distribution. During the aging process, standard deviation value increases significantly, which is also an indicator of deviation from standard normal distribution. At the final stage of aging process (Cycle #7), standard deviation value becomes 20 times bigger than the initial case (healthy motor).

The other statistical parameters do not differ as much as standard deviation. The probability density functions show the differentiation on these parameters by each aging cycle in Fig. 9 and the amplitude of data distribution increases.

The increase trend of standard deviation can be observed in Fig. 10 and it implies that the degradation of bearing accelerated after aging Cycle #3, which finally leads to bearing fault in the last cycle.
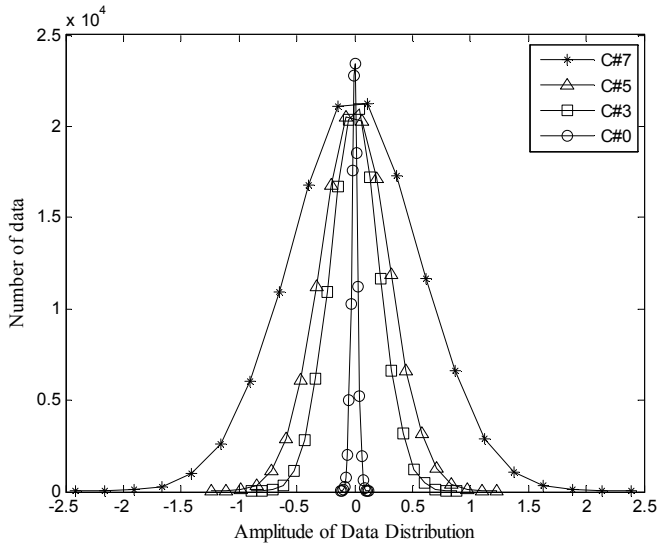
Fig. 9. Probability density functions of aging cycles No #0, 3, 5 and 7
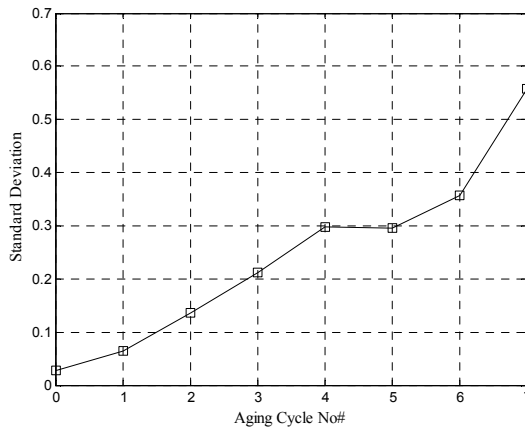(Case #0 - Healthy motor, Case #3 and Case #7 - Bearing fault)

Fig. 10. Standard deviation trend as a function of aging cycles

5. Entropy Approach for Vibration Signal Analysis

According to the Shannon Entropy definition given in Appendix C, entropy value, which is defined as a measure of uncertainty, will be helpful to understand the degree of degradation by calculating the amount of transferred data from initial case (healthy motor) to the last aging cycle (bearing fault) throughout the aging process [9].

It was stated in Section 4.2 that standard deviation is the parameter that undergone the most significant change during the aging process. Therefore regarding to the entropy definition, standard deviation can be the parameter which determines the probability value of each cycle at the aging process.

Thus there will be eight probability values in terms of following p_i definition:

$$p_i = \frac{\sigma_0}{\sigma_i} \tag{6}$$

1270

where σ_0 is standard deviation at the initial case (healthy motor), i is the aging cycle index ($i = 1, ..., 7$) for each aged state, and σ_i is standard deviation at the ith aging cycle. For instance, the probability value of first aging will be:

$$p_1 = \frac{\sigma_0}{\sigma_1} = \frac{0,0267}{0,0642} = 0,4155$$

In terms of physical meaning, p_i value determines the probability of being healthy, where also the probability of being faulty, q_i, is defined as below:

$$q_i = 1 - p_i + \varepsilon \tag{7}$$

where ε is a small constant value ($\varepsilon = 0.0001$).

Therefore, at the initial case (healthy motor), the probability of being healthy will be calculated as ($p_0 = 1$), as well as the probability of being faulty will be zero ($q_0 = 0$). Also, the probability of being faulty for the first aging cycle can be calculated as:

$$q_1 = 1 - 0,4155 + 0.0001 = 0,5846$$

At this point, Shannon Entropy definition, as given in Appendix C, will help to evaluate the entropy value of each aging cycle. Entropy value of the initial case, regarding the probability of being healthy state, will be zero as stated below:

$$H_{p1} = -p_1 \log_2(p_1) = 0.5265$$

also the entropy value of the initial case, regarding the probability of being faulty state, will be calculated as below:

$$H_{q1} = -q_1 \log_2(q_1) = 0.4527$$

Table 2 gives the probability values in terms of being healthy (p_i) and faulty (q_i) and also entropy values regarding probabilities of each aging cycles of the process.

Table 2. Probability and entropy values

Aging Cycle	p_i	q_i	H_{pi}	H_{qi}
C#0	1	0	0	0.0013
C#1	0,4155	0,5846	0,5265	0,4527
C#2	0,1968	0,8033	0,4616	0,2539
C#3	0,1253	0,8748	0,3755	0,1689
C#4	0,0895	0,9106	0,3116	0,1230
C#5	0,0903	0,9098	0,3133	0,1241
C#6	0,0746	0,9255	0,2793	0,1033
C#7	0,0478	0,9523	0,2097	0,0672

The trends of probability functions regarding aging cycles are provided in Fig. 11.

Calculated entropy values for each aging cycle are presented in Fig. 12 and Fig. 13. The figures indicate that the greater aging cycle, the greater probability of being faulty, the lower is the entropy value. It means that during the aging process the probability of being faulty increases and the uncertainty at being faulty state decreases which depends on the Shannon Entropy definition.

If the entropy variation between each aging cycle has been evaluated then it is possible to realize the amount of entropy which is transferred between aging cycles. Thus the entropy transfer rate ΔH can be defined as given in Eq. (2), Section 2. Here i is the number of aging cycle ($i = 1, ..., 7$). By this calculation, ΔH_i values in terms of fault prospect are given in Table 3 and shown in Fig. 14.
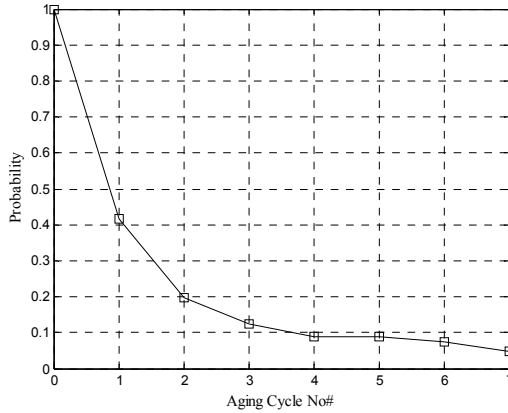
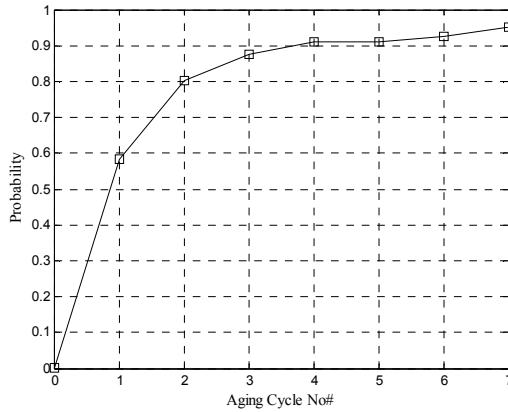**Fig. 11(a).** Probability function regarding state of being healthy

Fig. 11(b). Probability function regarding state of being faulty

From the point of being faulty prospect, the entropy transfer rate has the maximum value at the first aging cycle, which points out the maximum uncertainty about this state. After every aging cycle process, the calculated transfer rates between cycles decrease as like the entropy value in Fig. 14 and Table 3. This trend can also be expressed by a limit function regarding the probability of being healthy as given below:

$$\lim_{p \to 1} \Delta H(p) = 0 \tag{8}$$

Table 3. Entropy transfer rates between aging cycles

ΔH_1	ΔH_2	ΔH_3	ΔH_4	ΔH_5	ΔH_6	ΔH_7
0,452	0,199	0,085	0,046	0,001	0,021	0,036

Thus, when the figures in this section are evaluated together, it can be realized that, beginning with the fourth aging cycle:

• The probability of being faulty state has a value over 0.90 which is very close to 100 % failure.

• The entropy value reaches a saturated level under 0.15 bits at all the other cycles.

• The entropy transfer rate gets a small value under 0.05 bits which is converging to zero value.
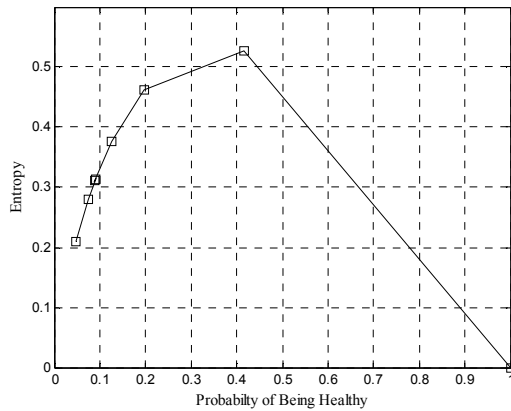
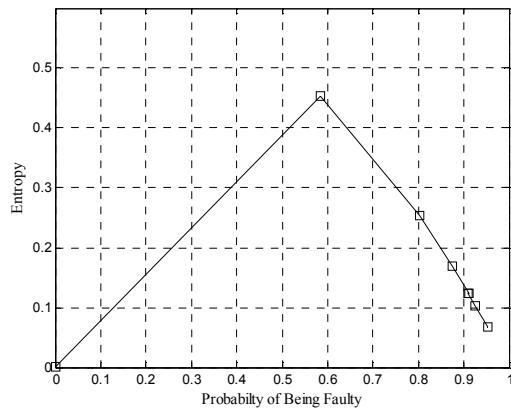**Fig. 12(a).** Entropy trend depending on probability of being healthy

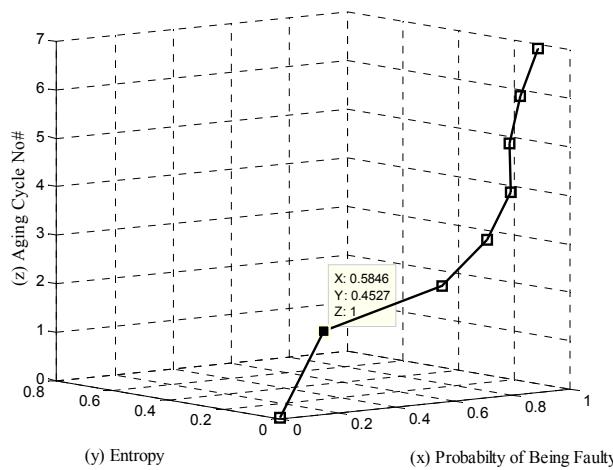**Fig. 12(b).** Entropy trend depending on probability of being faulty

Fig. 13. Entropy values regarding the probability of being faulty at each aging cycle

Therefore the fourth aging cycle can be determined as the remarkable stage of bearing degradation that can be considered significant.
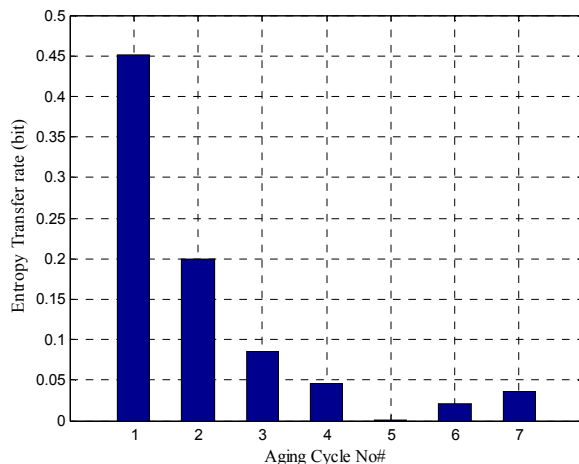
Fig. 14. Entropy transfer rates at each aging cycle

6. Discussion and Conclusions

The main purpose of this study was to analyze motor vibration signal data to maintain a fault detection approach due to bearing fault in an induction motor. Hence, an experimental setup was built to simulate the bearing fault state in an induction motor by an accelerated aging process. Motor vibration signal data collected from the experimental setup by properly installed accelerometers for totally 8 states of the motor. The first data set was for the initial case (healthy motor) and the other seven states refer to the aging process cycles, where the last cycle was for the faulty state of the motor bearing.

While investigating vibration data in time domain, it is clear that the magnitude of the signal increases after each aging cycle. Therefore eight sets of vibration data were examined by spectral analysis. It was established that frequency components between 1.5-4 kHz increase due to bearing degradation after each aging process cycle. Thus a Butterworth type high-pass filter was applied to examine the pure effect of these frequency components in the frequency band (>1.5 kHz). Power spectral density of the data for each aging cycle revealed that high frequency components above 1.5 kHz increase due to bearing degradation.

Statistical analysis has been conducted to the filtered vibration signal data sets. Four statistical parameters were determined: mean value, standard deviation, skewness and kurtosis. Standard deviation has undergone the most considerable change during aging process. Therefore, probability values of each aging cycle states have been calculated by the probability definition in (1) regarding the standard deviation parameters. According to these calculations, the probability of being healthy state has drawn a decreasing trend during the aging process in Fig. 11(a). During the accelerated aging process, the probability value of being healthy starts with 1.0 (100 % healthy) value and approaches to a lower rate (approx. 5 %) value at the last aging cycle, which indicates the bearing fault state.

Shannon Entropy approach has been applied to identify the bearing fault trend. Shannon Entropy is defined as a measure of uncertainty on a random signal data and it is a function of probability value for the motor states. All the calculation results regarding probability and entropy values are given in Table 2. The probability values are evaluated regarding both healthy and faulty states.

The probability of faulty state reaches the value over 0.90 after 4th aging cycle, which can be an alarm level for early fault detection. Finally, it reaches the value of 0.95, which clearly implies bearing fault.

1274

Also entropy regarding faulty state had the biggest value at the initial cycles with a decreasing trend as shown in Fig. 12. This result demonstrates that the uncertainty about motor bearing state decreases. After the 4th aging cycle, the value of entropy dropped down to a lower level of 0.15 bits, which can be an alarm level for the fault detection.

Finally, entropy transfer rate, between each aging cycles, has been calculated by the difference of entropy values. The examined data in Table 3 reveals that the entropy transfer rate also decreases gradually from the initial cycles to the last cycle. After the 4th cycle, the entropy transfer rate decreases below a small value of 0.05 bits, which also constitutes an alarm level for the fault detection.

In this study, all these figures regarding entropy approach state out a degradation trend for the motor bearing during the aging process. Thus, it becomes important to define a proper alarm level on these trends as an early fault detection process.

Appendix A. Frequency Domain - Spectral Analysis

The frequency features of a random signal can be identified generally by applying Fourier Transform, which is a continuous function that transforms the signal from time domain to frequency domain. General Fourier Transform definition is:

$$X(f) = \int_{-\infty}^{\infty} x(t) \cdot e^{-j2\pi ft} dt \tag{A.1}$$

where $X(f)$ is a complex transform of $x(t)$. t and f are real numbers, which are time variable in seconds and frequency variable in Hertz, respectively.

If it is defined in discrete form, DFT will be expressed as below by accepting $f = m\Delta f$ and $t = k\Delta t$, and assuming that $x(t)$ has nonzero values only at the times $t = k\Delta t$ for N values of k. Also $X(f)$ has non-zero values only at the frequencies of $f = m\Delta f$ for N values of m:

$$X(m\Delta f) = \sum_{k=0}^{N-1} x(k\Delta t) \cdot e^{(-j2\pi km/N)} \tag{A.2}$$

where $m = 0,\ 1,\ ...,\ (N-1)$ and here Δf and Δt are defined as frequency resolution and data sampling interval respectively.

Fast Fourier Transform (FFT) is a special version of DFT which is running more efficiently. In the case of DFT, N complex valued functions are computed by N^2 number of operations, but Cooley & Tukey performed an algorithm for computing DFT in number of $N \cdot \log_2 N$ where N is a power of 2, which is known as FFT [17, 18].

Power Spectral Density function measures the distribution of power of a random signal in the frequency domain. It is also the Fourier transform of autocorrelation function. Therefore the auto power spectral density of $x(t)$ is defined as [18]:

$$S_{xx}(f) = \frac{1}{N} |X(m\Delta f)|^2 \tag{A.3}$$

where $f = m\Delta f$.

Appendix B. Statistical Analysis

Generally, four basic statistical parameters are examined to analyze the features of a random signal. Two of these parameters are mean value (μ) and standard deviation (σ), which are defined as below regarding a collected data set $\{x_i\}$ with N, number of data points:

$$\mu = \frac{1}{N} \sum_{i=1}^{N} x_i \qquad (A.4)$$

$$\sigma = \sqrt{\frac{1}{N} \sum_{i=1}^{N} (x_i - \mu)^2} \qquad (A.5)$$

Mean value describes the location of distribution for the data set. Typically, the central value is the best value that describes the data. Also standard deviation is the square root of variance, which characterizes the variability of the data set.

Regarding the Gaussian (normal) probability distribution, two other parameters are concerned to expose the variation from normal distribution. They are known as skewness (c) and kurtosis (k) and defined as below:

$$c = \frac{\left[\dfrac{1}{N} \sum_{i=1}^{N} (x_i - \mu)^3 \right]}{\sigma^3} \qquad (A.6)$$

$$k = \frac{\left[\dfrac{1}{N} \sum_{i=1}^{N} (x_i - \mu)^4 \right]}{3\sigma^4} \qquad (A.7)$$

Skewness is a measure of symmetry for the collected data set and zero skewness is a characteristic property of the normal distribution. Positive skewness informs that the distribution is skewed at right side, and negative value informs that the distribution is skewed at left side of the centre.

The other parameter, kurtosis is a measure of flatness of the data set distribution. Regarding normal distribution, kurtosis value is 3 (three), whereas greater values imply "peaked" distribution and the lower values imply "flat" distribution [19].

Appendix C. Shannon Entropy Function

Entropy is defined as a measure of uncertainty and irregularity of a random signal. In the form of Shannon entropy, the expected value of the information being transferred in a block of data is computed in units of "bits". The mathematical definition of Shannon Entropy, H is presented below by a logarithmic equation with base 2:

$$H = -\sum_{i=1}^{n} p_i \log_2(p_i) \qquad (A.8)$$

Here i is the number of states ($i = 1, ..., n$) and p_i is the probability value for each index state [9, 20].

Acknowledgement

References

[1] **Bellini A., Filippetti F., Tassoni C., Capolino G. A.** Advances in diagnostic techniques for induction machines. IEEE Transactions on Industrial Electronics, Vol. 55, No. 12, December 2008, p. 4109-4126.

[2] **Nandi S., Toliyat H. A., Li X.** Condition monitoring and fault diagnosis of electrical motors - a review. IEEE Transactions on Energy Conversion, Vol. 20, No. 4, December 2005, p. 719-729.

[3] **Bonnett A. H.** Cause and analysis of bearing failures in electrical motors. IEEE Conference Publications, 1992, p. 87-95.

[4] **Bonnett A. H.** Root cause AC motor failure analysis with a focus on shaft failures. IEEE Transactions on Industry Applications, Vol. 36, No. 5, September/October 2000, p. 1435-1448.

[5] **Raison B., Rostaing G.** Investigations of algorithms for bearing fault detection in induction drives. IECON 02 - IEEE Conference Publications, 2002, p. 1696-1701.

[6] **Zhou W., Habetler T. G., Harley R. G.** Bearing condition monitoring methods for electric machines - a general review. SDEMPED 07 - IEEE Conference Publications, 2007, p. 3-6.

[7] **Stack J. R., Habetler T. G., Harley R. G.** Fault classification and fault signature production for rolling element bearings in electric machines. IEEE Transactions on Industry Applications, Vol. 40, No. 3, May/June 2004, p. 735-739.

[8] **Immovilli F., Bellini A., Rubini R., Tassoni C.** Diagnosis of bearing faults in induction machines by vibration or current signals - a critical comparison. IEEE Transactions on Industry Applications, Vol. 46, No. 4, July/August 2010, p. 1350-1359.

[9] **Seker S., Onal E.** Entropy transferred by aging process in electrical motors. International Review of Electrical Engineering (I. R. E. E.), Vol. 5, No. 4, 2010, p. 1550-1554.

[10] **Rocci P.** Calculations of system aging through the stochastic entropy. ISSN 1099-4300, Entropy 2006, Vol. 8, p. 134-142.

[11] **Jay M. E., Russel J. K., David W. S., Gary L. S.** Effect of PWM inverters on AC motor bearing currents and shaft voltages. IEEE Transactions on Industry Applications, Vol. 32, No. 2, March/April 1996, p. 250-259.

[12] **Ferreira F. J. T. E., Trovao J. P., Almedia A. T.** Motor bearings and insulation system condition diagnosis by means of common-mode currents and shaft-ground voltage correlation. Proceedings of the 2008 International Conference on Electrical Machines, 2008, Paper ID 1315.

[13] IEEE Std. 117/1974/ANSI C50.32-1976. IEEE Standard Test Procedure for Evaluation of Systems of Insulation Materials for Random-Wound AC Electric Machinery, 1976.

[14] U. L. Inc. Proposal of the Fifth Edition of the Standard for Systems of Insulation Materials – General, UL 1446, 1997.

[15] **Seker S., Ayaz E.** A reliability model for induction motor ball bearing degradation. Electric Power Components and Systems, Taylor&Francis, 2002, p. 639-652.

[16] **Seker S., Ayaz E., Upadhyaya B. R., Erbay A. S.** Analysis of motor current and vibration signals for detecting bearing damage in electric motors. MARCON 2000, Maintenance and Reliability Conference, Knoxville, May 2000.

[17] **Senguler T., Karatoprak E., Ayaz E., Gullulu S., Seker S.** Entropy approach using PCA for sequential accelerated aging process in electric motors. The 16th IEEE International Symposium on Diagnosis for Electric Machines, Power Electronics and Drives, Poland, 2007, p. 501-505.

[18] **Romberg T. M., Black J. L., Ledwidge T. J.** Signal Processing for Industrial Diagnostics. Wiley J., 1996.

[19] **Cowen G.** Statistical Data Analysis. Oxford Press, 1998.

[20] **Shannon C. E.** A mathematical theory of communication. The Bell System Technical Journal, Vol. 27, July 1948, p. 379-423.

[21] **Taylor J. K., Cihon C.** Statistical Techniques for Data Analysis. Champman & Hall, 2004.

[22] **Heng R. B. W., Nor M. J. M.** Statistical analysis of sound and vibration signals for monitoring rolling element bearing condition. Applied Acoustics, Vol. 53, No. 1-3, 1998, p. 211-226.

[23] **Oppenheim A. V., Schafer R. W.** Digital Signal Processing, Prentice Hall of India, 2001.

[24] **Hershy D.** Entropy Theory of Aging Systems, Imperial College Press, 2010.

[25] **Bevensee R. M.** Maximum Entropy Solutions to Scientific Problems. P T R Prentice Hall, 1993.